

UNIVERSITY OF CALIFORNIA,
MERCED

Cell Type-specific Analysis of Gene Expression
in an *In Vitro* Model of Neurogenesis

THESIS

submitted in partial satisfaction of the requirements
for the degree of

MASTER OF SCIENCE
in Quantitative and Systems Biology

by

Sophia M. Tang

Thesis Committee:

Assistant Professor David H. Ardell, Chair

Assistant Professor Michael D. Cleary

Assistant Professor Marcos E. García-Ojeda

Assistant Professor Kara McCloskey

2010

DEDICATION

To

my parents and friends

in recognition of their enduring love and support

TABLE OF CONTENTS

	Page
LIST OF FIGURES	iv
LIST OF TABLES	vi
ACKNOWLEDGEMENTS	vii
ABSTRACT OF THE THESIS	viii
CHAPTER 1: INTRODUCTION	1
Summary of <i>in vivo</i> embryonic and adult neurogenesis	1
An <i>in vitro</i> model of neurogenesis	2
Heterogeneous differentiation	3
Temporal dependence	3
Niche communication	5
Cell signaling	6
Identification of cell type-specific mRNAs	7
Research aim of thesis project	10
CHAPTER 2: METHODS	11
Ubiquitous UPRT expression vectors	11
Cell type-specific UPRT expression vectors	13
TU-Tagging methods	14
P19 cell culture and transfection methods	16
CHAPTER 3: RESULTS AND DISCUSSION	19
TU-tagging in HeLa as control	19
TU-tagging P19 culture	21
P19 neural differentiation	23

CHAPTER 4:	FUTURE DIRECTIONS	26
	TU-tagging in P19 tissue culture using nestin-UPRT vector	26
	TU-tagging in primary NSCs and niche co-culture	28
REFERENCES		30

LIST OF FIGURES

	Page
Figure 1: Model of Neurogenesis	1
Figure 2: Neurogenesis in the Developing Embryos and the Adults over Time	2
Figure 3: Fez Family Zinc-Finger (Fezf2) is a Progenitor Temporal Transcription Factor in NSCs of the Developing Cerebral Cortex in Vertebrates	5
Figure 4: Cell Signals that Regulate Homeostasis in the SVZ Niche and the SGZ Niche	6
Figure 5: The UPRT Pathway	9
Figure 6: Diagram of the TU-Tagging Method to Extract Cell Type Specific mRNAs	10
Figure 7: Vector Map of pIRES	11
Figure 8: Pathway from sUMP to sUDP to sUTP	12
Figure 9: Flow Chart for P19 RA Neural Differentiation and Cell Marker Staining Experiment	17
Figure 10: Flow Chart for TU-tagging Experiments in P19 Culture	18
Figure 11: TU-Tagging Blot in HeLa Tissue Culture	20

Figure 12: TU-Tagging Blot in P19 Tissue Culture	21
Figure 13: HA Staining of pcDNA3.3-TOPO-HA-UPRT Transfected P19 Cells	23
Figure 14: Immunocytochemistry from P19 Neural Differentiation	24
Figure 15: Flow Chart of Future Experiments to Analyze NSC-specific mRNAs from P19 Neural Differentiation using Nestin-UPRT Vector	27
Figure 16: Flow Chart of Future TU-Tagging Experiments on the Co-Culture of Primary NSCs with Endothelial or Astrocytes Niche Cells	28

LIST OF TABLES

	Page
Table 1: The Most Common Markers used in the Literature	4
Table 2: Data on the Frequency of Cell Types from P19 Neural Differentiation	25
Table 3: Markers for NSCs, Neurons, Astrocytes and Oligodendrocytes	27

ACKNOWLEDGEMENTS

I would like to thank my advisor Professor Mike Cleary for training me to conduct experiments independently, having discussions about my data and results, giving me opportunities to practice giving scientific presentations, and providing comments on my writings and presentations. I would also like to thank each of my committee members, Dr. Ardell, Dr. García-Ojeda and Dr. McCloskey for feedbacks on my thesis project. I want to thank my colleagues in the Cleary lab for all the moral support and help. Thanks to the fellow graduate students in the Stem Cell Suite of the García-Ojeda lab, Pallavicini lab and Manilay lab, for helpful discussion and sharing protocol and reagents. I wanted to thank the graduate coordinator Carrie King at the School of Natural Sciences for help with many questions surrounding obstacles with completing my degree. And I thank Randall Hart for editing my thesis and help with practicing presentations.

The nestin-GFP vector for the nestin-UPRT vector came from Nibedita Lenka of the National Center for Cell Science in India. The GFAP vector and Tuj1 vector came from Fred Gage at the Salk Institute. The project was funded by a generous grant from the California Institute for Regenerated Medicine (CIRM) for developing the TU-tagging technique. Thanks for the graduate training in UC Merced.

ABSTRACT OF THE THESIS

The project attempts to answer the following question: What are the neural stem cell (NSC) transcription factors (TFs) that determine neurogenesis and those that determine astrogenesis? NSCs co-exist with other neural cell types during differentiation and communicate with other cells in the NSC niches. Furthermore, expressions of the NSC TFs are time dependent. These conditions make it very challenging to analyze TFs of NSCs. The technique I will use to address the challenge is called TU-tagging, which utilizes the UPRT enzyme from *Toxoplasma gondii* that is not found in mammalian cells to incorporate a thio-tag into the mRNA only in a specific cell type. A long-term aim is to apply TU-tagging to extract cell type-specific mRNAs in the *in vitro* model of neural differentiation. In my work, preliminary experiments have been performed and reagents have been generated to help meet this goal. Ubiquitous and cell type-specific UPRT expression vectors for TU-tagging have been made and were used to validate the method using a P19 cell line that is a traditional model of neural differentiation.

CHAPTER 1: INTRODUCTION

SUMMARY OF *IN VIVO* EMBRYONIC AND ADULT NEUROGENESIS

Neural stem cells (NSCs) are characterized by their potential of self-renewal and differentiation into all neural lineages: neurons, astrocytes and oligodendrocytes of various types (Figure 1). Altogether, they serve the complex functionality of the central nervous system. In mammals, neurogenesis begins in the embryo and continues into adulthood at the subventricular zone (SVZ) and at the hippocampal subgranular zone (SGZ), (Figure 2, adapted from Kriegstein and Alvarez-Buylla 2009). At any stage, either in the embryo or in the neurogenic regions of the adult brain (SVZ and SGZ), NSCs divide asymmetrically, thereby one self-renews as a NSC and the other eventually differentiates into a mature neural lineage (neuron, astrocyte or oligodendrocyte), usually via an intermediate progenitor cell (IPC). More mature cells (IPC and differentiated cells) divide symmetrically. Terminally differentiated neurons do not divide in the adults. In the adults, after injury or neurodegeneration, but only at the neurogenic regions, quiescent NSCs proliferate, differentiate, migrate, mature and integrate into the existing neural circuitry (Svendsen and Smith 1999). However, neurons are permanently lost at the non-neurogenic regions after damage. For therapeutic applications, this makes the treatment of neural injury and neurodegeneration challenging in adults.



Figure 1: Model of Neurogenesis. An NSC has the potential to self-renew and differentiate into any of the three neural lineages: oligodendrocyte, neuron, and astrocyte.

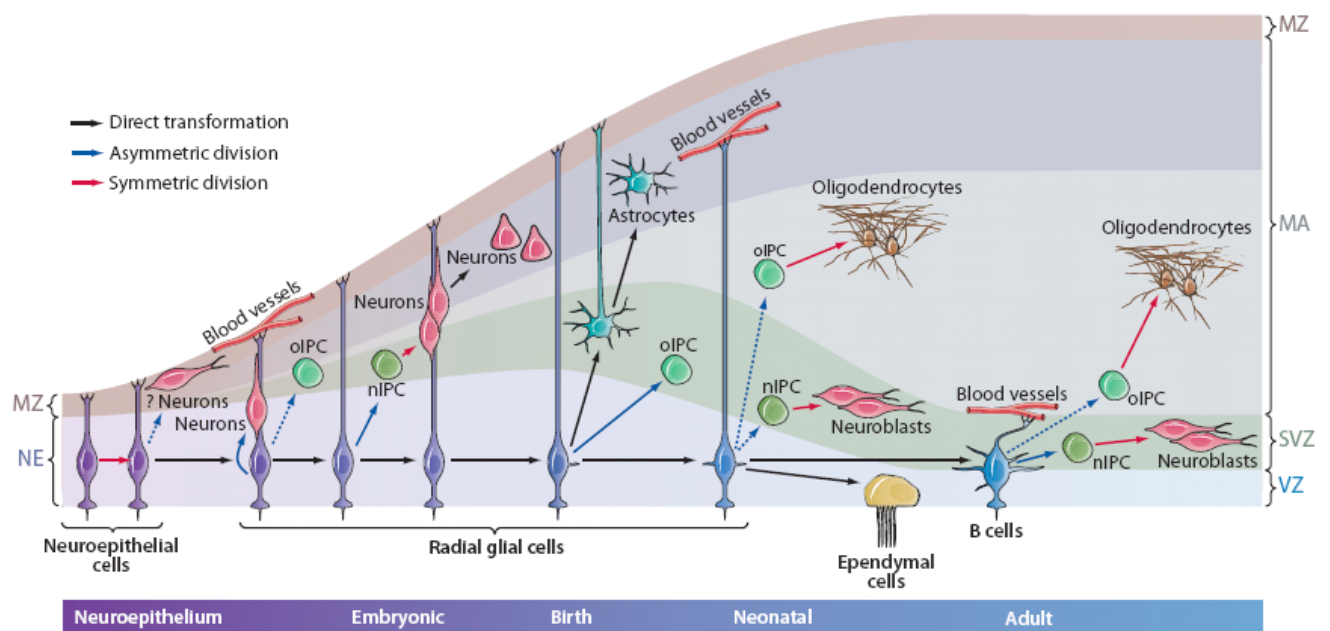


Figure 2: Neurogenesis in the Developing Embryo and the Adult over Time. NSCs divide asymmetrically, one self-renews and the other eventually differentiates into a neuron or astrocyte or oligodendrocyte, usually via an intermediate progenitor cell (IPC). Immature differentiated cells migrate along the rostral migratory stream (RMS) in the SVZ and to the granular cell layer of the dentate gyrus in the hippocampus. Figure adapted from Kriegstein & Alvarez-Buylla, *Annu Rev Neurosci* 2009.

AN IN VITRO MODEL OF NEUROGENESIS

Understanding how NSCs generate different cell types carries a scientific merit, while applying this to neurogenesis provides insights into medical treatments. The *in vitro* model offers two main benefits. First, it allows us to control the experimental condition and enables us to simplify the system and isolate the system from interference. This will provide insights into the mechanism and a model of the biology in embryos and in adult cells. Second, from the application point of view, stem cell therapy offers a promising medical alternative to pharmaceuticals and surgical intervention, for its wide range of therapeutic strategies (Svendsen and Smith 1999; Lie, Song et al. 2004). For human therapy, NSCs should not be directly delivered into humans because they might proliferate and cause cancer. Therefore, NSCs should be directed *in vitro* to differentiate into a given cell type. However, NSC differentiation naturally gives rise to a heterogeneous cell population. Therefore we have to understand the molecular and cellular mechanism that directs NSCs to produce neurons versus astrocytes versus oligodendrocytes, and even the classes of neurons such as glutamatergic, GABAergic, dopaminergic, or cholinergic neurons.

From the stem cell therapy stand point, embryonic stem (ES)-derived NSCs are preferred over somatic NSCs obtained from embryos or adult brains. One of the reasons is that ES-derived

NSC can be maintained in an undifferentiated state for 6 months or more, while somatic NSCs can be maintained in an undifferentiated state for less than a month (Colombo, Giannelli et al. 2006). ES-derived NSCs are similar to somatic NSCs in that they share maintenance pathways such as Wnt, Notch and Hedgehog, and less than 2% mRNA transcripts are changed significantly from NSCs (Colombo, Giannelli et al. 2006). The major difference is perhaps that ES-derived NSCs produce more neurons(60%) while somatic NSCs produce more astrocytes (72%)(Aiba, Sharov et al. 2006). Adult NSCs also produce more astrocytes (64%) than neurons (28%)(Colombo, Giannelli et al. 2006). Therefore, we need to understand how to direct NSCs to produce the type of neural cell type we need. Furthermore, we need to understand the communication between NSCs and their natural niche environment (discussed in the following section), so that by recreating the niche *in vitro*, NSCs produce mature neural cells that mimic the characteristics and compatibility after the neural cell types are transplanted and integrated into the host niche.

HETEROGENEOUS DIFFERENTIATION

NSC differentiation naturally gives rise to a heterogeneous cell population both *in vivo* and *in vitro*. The population mixture is composed of NSCs that proliferate and self-renew, intermediate progenitor and transient amplifying cells, and differentiated progenies (neurons, astrocytes, oligodendrocytes) (Miller and Gauthier-Fisher 2009). This heterogeneity makes it difficult to study the gene expression of an individual cell type, such as NSCs.

TEMPORAL DEPENDENCE

The challenges of both *in vivo* and *in vitro* studies lie not only on the fact that NSC differentiation gives rise to a heterogeneous population, but also that the proportion of different neural cell types changes over time. In one of the NSCs *in vitro* experiments, NSCs were co-cultured with niche endothelial cells (ECs) placed in a transwell setting for 7 days(Shen, Goderie et al. 2004). ECs were removed and NSCs were allowed to differentiate for two weeks. On the 11th day, the population contained a mixture of self-renewed NSCs (as indicated by immunostain of LeX which is specific to NSCs) and newly generated neurons (as indicated by immunostain of β -tubulin which is specific to neurons). On the 14th day, astrocytes (as indicated by immunostain of GFAP which is specific to astrocytes) were newly generated. Two weeks later, the proportion of combined NSCs and neurons were reduced compared to those on the 11th day. The most common markers used in the literature for each cell type are listed in Table 1.

Table 1: The most common cell markers used in the literature to identify NSCs and their progeny

Cell types	Markers	References
NSCs	Nestin, SOX2, LeX	(Shen, Goderie et al. 2004), (Cheng, Pastrana et al. 2009)
Neurons	MAP2, MBP, Tuj1, NeuN	(Song, Stevens et al. 2002), (Cheng, Pastrana et al. 2009)
Astrocytes	GFAP	(Song, Stevens et al. 2002)
Oligodendrocytes	Olig2	(Colombo, Giannelli et al. 2006)

This temporal control of neurogenesis is shown in both vertebrates and insects, and they may share the same mechanism (Jacob, Muraugue et al. 2008). In *Drosophila*, there is a set of progenitor temporal transcription factors (progenitor TTFs) that vary in expression over the length of development: first Hunchback (Hb), then Kruppel (Kr) and Pdm, followed by Castor (Cas). When a progenitor divides asymmetrically, the later born progeny has different post-mitotic TTFs compared to the early sibling. Besides this birth-order, switching factors and competence factors also regulate formation of the diverse neural lineages. Switching factors directly or indirectly regulate progenitor TTFs. They can be components that regulate cell cycle or those that determine whether the NSCs produce neurons versus glial cells. The competence factors are intrinsic factors and extrinsic factors that the progenitors can respond to only within a given developmental time window

In vertebrates, the Fez family zinc-finger 2 (Fezf2) has been shown to be a progenitor TTF (Jacob, Muraugue et al. 2008). The cerebral cortex is a great example for studying temporal regulation because it contains a diverse number of cell types generated at different time and forms six layers. First the superficial layer is formed (I or SP). Then the layers are formed in an inside-out order (VI towards II) (Figure 3c). In the wildtype mouse embryogenesis, Fezf2 is expressed in the progenitor early during development, when neurons in the deep layers (VI and V) are formed. Later in development, Fezf2 is not expressed and neurons are generated in outer layers (IV, III and II) (Figure 3a). When Fezf2 is over-expressed causing it to express beyond its regular time window, neurons in the outer layers express Ctip2 gene typical of the deeper layer (V) (Figure 3b top). On the other hand, when Fezf2 is deleted, neurons in the deeper layer express Satb2 typical of the outer layers (IV, III and II).

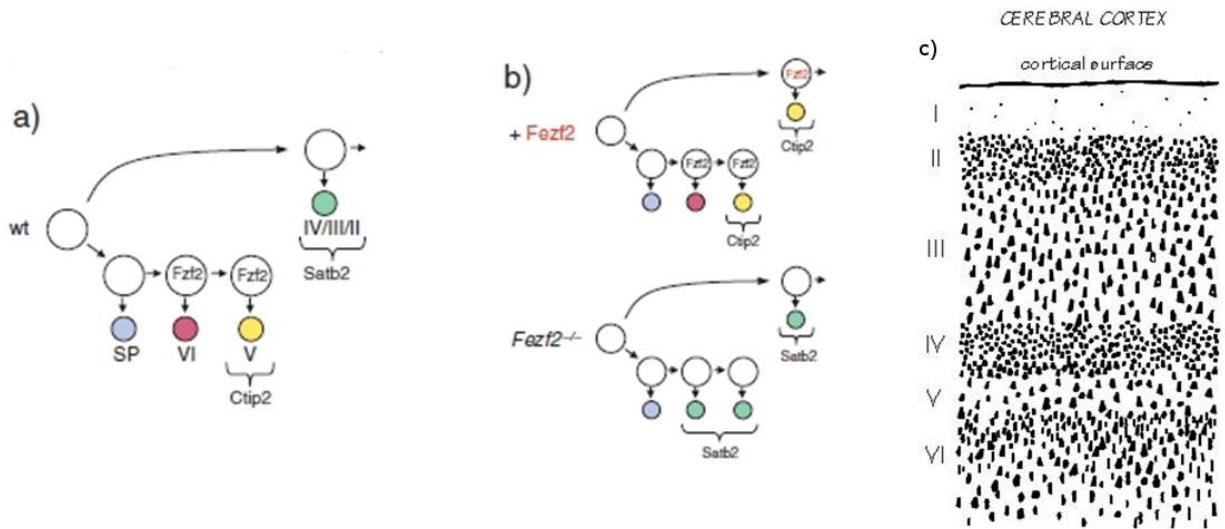


Figure 3: Fez Family Zinc-Finger (Fezf2) is a Progenitor Temporal Transcription Factor in NSCs of the Developing Cerebral Cortex in Vertebrates. In wildtype mouse embryogenesis, Fezf2 is expressed early during development (a). Neurons express abnormal markers at respective layers when Fezf2 is over-expressed (b top) or deleted (b bottom). Spatial structure of the six layers in the cerebral cortex (c). Figure adapted from Jacob, Maurange et al. 2008.

Temporal regulation is also observed *in vitro*. When mouse embryonic stem cells were cultured in the presence of sonic hedgehog inhibitor, they generated neurons which expressed cortical markers in a sequence that recapitulates native corticogenesis (Gaspard, Bouchet et al. 2008). Similar to *Drosophila*, this suggests that the core mechanism which gives rise to neuronal diversity is intrinsic cues driven.

NICHE COMMUNICATION

The primary molecular difference of embryonic versus adult neurogenesis is perhaps the signals to which NSCs respond. Independent investigations suggest that embryonic NSC fate is more controlled by intrinsic cues (Gaspard, Bouchet et al. 2008; Jacob, Maurange et al. 2008), while adult NSC fate is more controlled by extrinsic cues from the niche cells (Lie, Song et al. 2004). ECs, astrocytes and ependymal cells have been demonstrated to be the niche cells for adult NSCs (Jacob, Maurange et al. 2008; Miller and Gauthier-Fisher 2009). ECs form the lining of the blood vessels and are in direct contact with the NSCs. The evidence that they are niche cells is shown in an *in vitro* study (Shen, Goderie et al. 2004). NSCs were co-culture with ECs placed in a transwell. ECs secrete soluble factors that enhance NSCs proliferation and neuron production as compared to NSCs cultured alone in the control experiment. Astrocytes are generated from the NSC pool and they provide nutrient to neurons and help with synapsis. The evidence that astrocytes are niche cells is based on another *in vitro* study (Song, Stevens et al.

2002). The neurogenic property of NSCs co-cultured with astrocytes depends on the origin of the astrocytes. When co-culture with astrocytes taken from the neurogenic region (e.g. hippocampus), the NSC is neurogenic, as indicated by Map2ab immunostain for neurons. When co-culture with astrocytes taken from the adult spinal cord, the co-culture is non-neurogenic. Ependymal cells are found to be the niche cells in the SVZ (Miller and Gauthier-Fisher 2009).

The niche extrinsic cues are also demonstrated in a number of transplantation experiments. When NSCs originally from the SGZ are transplanted back, granule cell neurons are produced (Suhonen, Peterson et al. 1996). However, if they are transplanted to the SVZ then interneurons are produced.

Hypoxia was also found to create a niche condition that affect neurogenesis. In the deeper layers of the brain where the oxygen concentration is typically low, NSCs are maintained to be undifferentiated and proliferation is enhanced. While in other parts of the body where oxygen levels are higher, proliferation is decreased and glia formation is increased (Giese, Frahm et al. 2010).

CELL SIGNALING

Neural cell fate is regulated in a spatial manner in the niche. In the SVZ, NSCs express BMP (bone morphogenic protein) which directs glial fate (Figure 4a) (Lie, Song et al. 2004). Meanwhile, the niche ependymal cells secrete BMP antagonist, noggin, and promote neuron formation. In the SGZ, NSC niche hippocampal astrocytes express Wnts, which promote neurogenesis (Figure 4b). In the mean time, NSCs secrete Wnt antagonist, sFRP3, to balance not having excess neurons. NSCs co-exist with many cell types in their microenvironments in a developing fetus, adult SVZ and adult SGZ. The niches encompass of different types of stem cells, progenitor cells, and mature neural cells, also cells from the vasculature, the ventricular zone, the marginal zone, and the extracellular matrix (ECM) (Kriegstein and Alvarez-Buylla 2009; Miller and Gauthier-Fisher 2009).

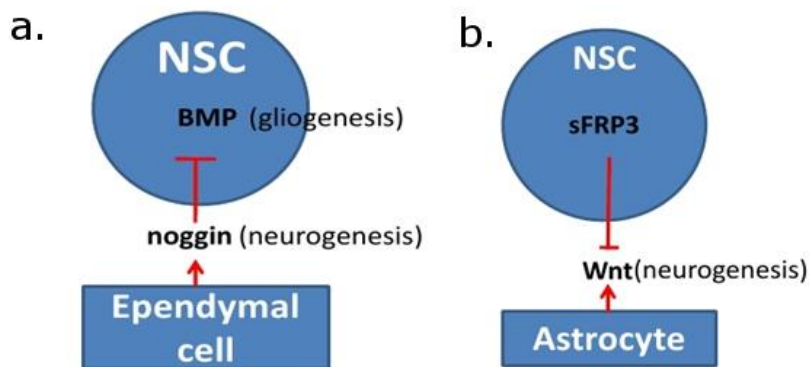


Figure 4: Cell Signals that Regulate Homeostasis in the SVZ Niche (a) and the SGZ Niche (b).

A number of signaling pathways have been identified that regulate NSC neurogenesis (Lie, Song et al. 2004; Aiba, Sharov et al. 2006; Colombo, Giannelli et al. 2006). The more studied ones are Notch, Wnt, mitogen activated protein kinase (MAPK), and growth factors activating signals such as by basic fibroblast growth factor (bFGF-2), insulin-like growth factor (IGF), and epidermal growth factor (EGF). Notch signaling maintains neural stem cell fate, the Wnt- β -catenin pathway promotes proliferation and neuron production, while the MAPK pathway enhances proliferation in ES-derived NSCs. Interactions with ECM promote proliferation, such as FGF-2, EGF, IGFI, IGFII and sonic hedgehog (Shh).

Some of the signaling pathways that regulate neuron versus glia production during the differentiation process have been identified through transplant experiments in rodents. BMP-Smad and JAK/STAT pathways promote astrocyte formation and inhibit neuron and oligodendrocyte formation upon spinal cord injury in mice (Xiao, Du et al. 2010). Myelination is enhanced in injured rat spinal cord post transplantation of human NSC cell line (F3) overexpressing Olig2—an essential helix-loop-helix transcription factor for oligodendrocyte development—by activating Nkx2.2 (Hwang, Kim et al. 2009; Islam, Tatsumi et al. 2009). Deletion of murine MAPK1/ERK2 gene in neural progenitor cells *in vivo* prevents neuron generation and results in astrocyte formation upon gliogenic stimuli (Samuels, Karlo et al. 2008).

IDENTIFICATION OF CELL TYPE-SPECIFIC mRNAs

The goal of this project is to discover new cell type-specific genes that regulate neurogenesis. Furthermore, we hypothesize that there are more transcription factors that determine NSC neural-fate and, astrocyte-fate when NSCs communicate with their niche cells. NSCs give rise to neurons and astrocytes, and astrocytes in turn are niche cells for the NSCs (Wurmser, Palmer et al. 2004). NSC heterogeneous differentiation, niche communication, and temporal dependence make it difficult to analyze gene expression of the NSCs.

All cell types of an individual have the same DNA coding. What makes them unique is RNA transcription (i.e. gene expression), which is regulated temporally and spatially. The dynamic is more complex when different cell types are communicating with each other during differentiation and with their microenvironment (i.e. the niche). Cell type-specific gene expression profile is more informative than that from the whole organism or the whole tissue, however it has not been feasible until recently.

One most widely utilized cell type-specific method up to day is fluorescence activating cell sorting (FACS), in which a specific cell type is isolated from a population mixture of cells or a tissue, and its gene expression is analyzed (Parker, Anderson et al. 2005). While most data and results of the previous literature are based on gene expression obtained using this method, caution should be taken as physical separation might change gene expression in unknown ways. This is more challenging for neural cells since they are more physically connected and intertwined. Since FACS sorts cells using an antibody to detect cell type marker expressed on

the surface of the cell, it is necessary to know the cell markers for a specific cell type. This information is not known for all cell types so this procedure is not always available.

An alternative approach is to create a tag for the RNA of a specific cell type which grows in a heterogeneous population. One method of this approach is known as “TU-tagging” (Cleary, Meiering et al. 2005), that allows extraction of a specific transcript from a cell type. This is the method used in our neurogenesis studies. It utilizes *Toxoplasma gondii*'s enzyme UPRT and the substrate 4-thiouracil (4-TU), to incorporate a thio-tag onto the uracil monophosphate (UMP) (Figure 5). The thio-tag is subsequently added onto the RNA chains as they are being synthesized. This cell type-specific tagged RNA can then be labeled and purified for gene expression analysis.

Another method of this approach expresses EGFP-L10a in a defined cell population of transgenic mice. Thus, EGFP is fused onto the large subunit of ribosomes. The EGFP tag is transferred to the RNA during translation. The cell type-specific RNA is purified using anti-EGFP beads (Heiman, Schaefer et al. 2008). The major difference of TU-tagging versus ribosome tagging is that, TU-tagging works prior to transcription while ribosome tagging works during translation.

The uracil phosphoribosyltransferase (UPRT) gene, taken from *Toxoplasma gondii*, is not found in mammalian cell lines. Therefore, it can be incorporated into mammalian cell lines and genetically manipulated to express UPRT only in the cell type of interests. After some time of UPRT expression, the cells are fed with 4-thiouracil (a thio group added to the 4th position of uracil, U) for four hours. The UPRT enzyme transfers the sugar group of PRPP (phosphoribose) to the substrate 4-thiouracil (4-TU) and converts it into 4-thiouridine 5-monophosphate (sUMP) (Figure 5). sUMP is then converted into sUDP and then into sUTP. The RNA polymerase incorporates this thio-attached uridine on the RNA chain, which does not normally contain a thio group. The thio group can be used for labeling and purification of the mRNAs (Figure 2b). We have shown that when UPRT containing *Toxoplasma* infects a human cell line, only *Toxoplasma* RNAs are labeled and human RNAs are not labeled (Cleary, Meiering et al. 2005).

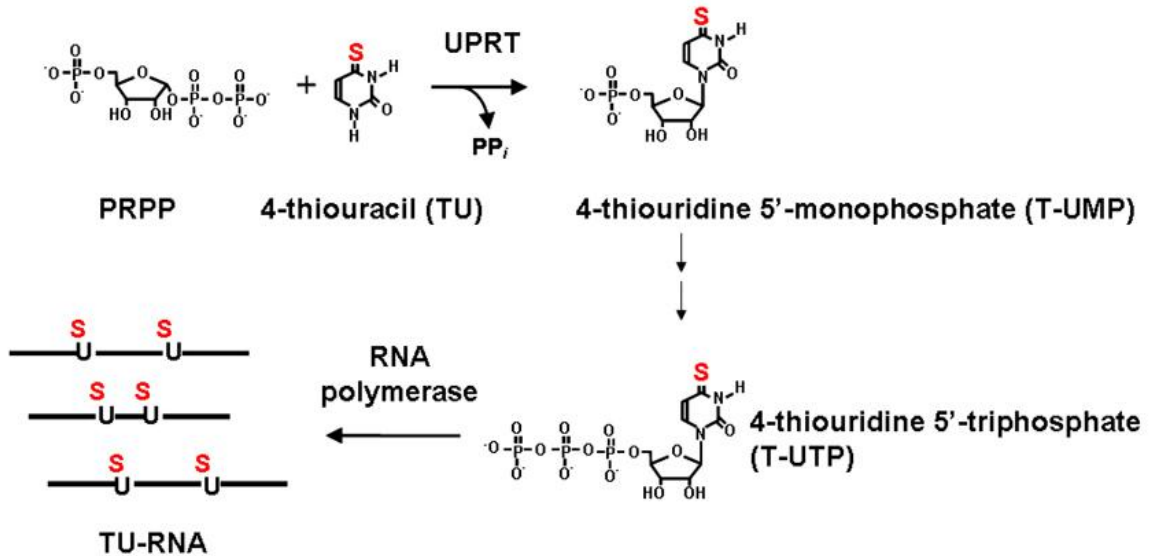


Figure 5: The UPRT Pathway. UPRT incorporates 4TU and phosphoribose of the PRPP, forming a UMP that contains a thio group. The thio-tagged is added to RNA during subsequent reactions.

The cell type-specific TU-Tagging method works as follows. In a heterogeneous population, one of the cell types expresses UPRT driven by a cell type-specific promoter (Figure 6). In the case where the mRNA will be extracted from NSCs, the nestin-UPRT vector will be transfected into the NSC. The other cell types, such as embryonal cancer cell line P19, neurons, astrocyte, oligodendrocytes, fibroblasts and niche cells, do not express UPRT so their RNA will not be TU-tagged. The Northern blot procedure to isolate the RNA is as follows, it is extracted from the cell using a Trizol preparation, then it is biotinylated, run through a gel and transferred onto a membrane. Alternatively, the biotinylated RNA is loaded onto a membrane via a vacuum facilitating positive pressure. The membrane is incubated in solution containing streptavidin-HRP. Unbound streptavidin-HRP is washed away. Only the cell type that expresses UPRT will have its RNA tagged with the Thio group which bonds with streptavidin-HRP. The HRP (horseradish peroxidase) enzyme oxidizes the ECL substrate using hydrogen peroxide as the oxidizing agent. The oxidation reaction is accompanied by emission of light and the light was detected on a film. The non-cell type-specific RNAs will not be detected.

The biotinylated mRNA can also be purified using a column of streptavidin beads that bind to the thio-tagged mRNA. The purified cell type-specific mRNA can be used to produce cDNA, which in turn can be used in quantitative PCR. The cell type-specific mRNAs can also be amplified and hybridized for microarray analysis.

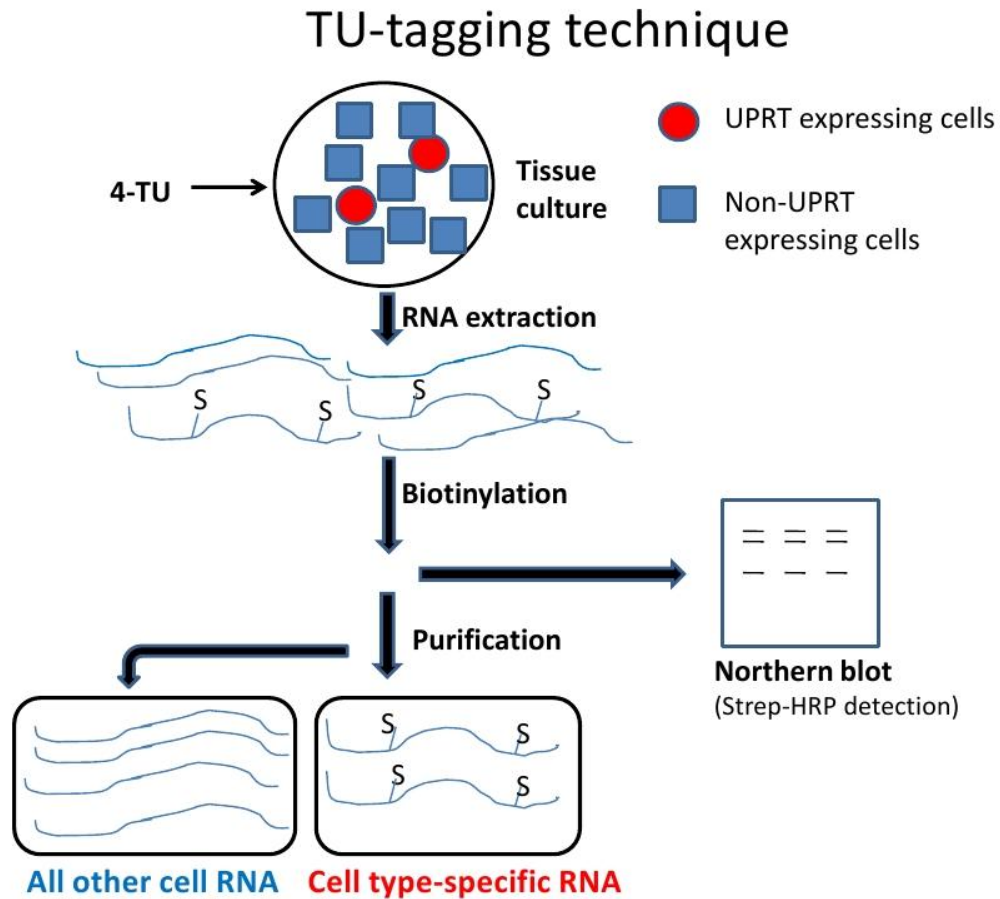


Figure 6: Diagram of the TU-Tagging Method to Extract Cell Type Specific mRNAs in the Heterogeneous Population in a Differentiation Experiment or a Niche Co-Culture Experiment.

RESEARCH AIM OF PROJECT

A long-term aim is to apply TU-tagging to extract cell type-specific mRNAs in the *in vitro* model of neural differentiation. In my work, preliminary experiments have been performed and reagents have been generated to help meet this goal. Ubiquitous and cell type-specific UPRT expression vectors for TU-tagging have been made and were used to validate the method using a P19 cell line that is a traditional model of neural differentiation.

CHAPTER 2: METHODS

I made two types of expression vectors. One type gives expression of UPRT ubiquitously (all cell types, e.g. stem cells, progenitors, mature neurons and astrocytes), another type gives expression of UPRT only in a specific cell type (neural stem cells, neurons, or astrocyte). Expression of the first type is driven by a potent cytomegalovirus immediate early enhancer-promoter (CMVie), which is found in all cell types and thus all cell types express UPRT. Expression of the second type is driven by a promoter using a cell marker for the cell type of interests (nestin for NSCs, Tuj1 for neurons, and GFAP for astrocytes).

UBIQUITOUS UPRT EXPRESSION VECTORS

UPRT-IRES-UPRT

Two copied of UPRT were cloned, one before and one after the IRES (internal ribosome entry site) sequence in the pIRES vector (Clontech, Figure 7). A gene added to the vector (UPRT in our project) generally has a stop codon. Therefore, translation generally stops after the first copy of UPRT. The IRES sequence allows an additional ribosome to bind to it and allows translation of the second copy of UPRT in the same vector.

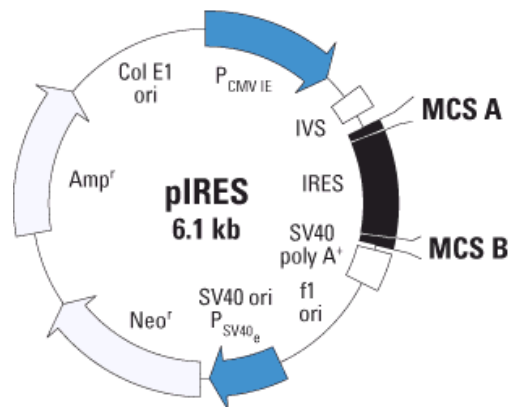


Figure 7: Vector map of pIRES, backbone of pIRES-UPRT.

pIRES-UPRT

Initially, the UPRT-IRES-UPRT vector was to be made using the conventional restriction digest method, but that did not appear to be successful. However, the topo method had a much higher success rate. The topo method works as follows (Invitrogen). A single deoxyadenosine (A) is added to the 3' end of the PCR product during each PCR cycle by *Taq* polymerase. The linearized TOPO vector has a single thymidine (T) at the 3' end and a covalently bound topoisomerase I from *Vaccinia* virus. The T and A complement with each other, while

topoisomerase facilitates the ligation. The tyrosyl residue (Tyr-274) of the topoisomerase I attacks the 3' phosphodiester backbone of the TOPO vector. The energy is conserved to form a covalent bond with the 5' hydroxyl of the PCR product, and topoisomerase is released. The TOPO vector has a CMVie promoter. The first copy of UPRT was cloned into a TOPO vector and was then cloned into Site A of the pIRES vector (before the IRES sequence). The second copy of UPRT was cloned into a TOPO vector but has not been cloned into the pIRES vector (Site B).

This pIRES-UPRT vector has been used in our tissue culture experiments and has been proven to label RNAs. Furthermore, our experiments show that the pIRES-UPRT has a higher TU-tagging efficiency than the pcDNA3.3- TOPO-HA-UPRT (described below) in HeLa cells (an immortalized cervical cancer cell line) and in P19 cells by one fold. One possibility is that the pcDNA3.3-TOPO- HA-UPRT vector contains a HA tag, and may reduce expression of UPRT. Another possibility is that the synthetic intron IVS of the pIRES vector stabilizes mRNA of UPRT, therefore enhances TU-tagging labeling.

pcDNA3.3- TOPO-HA-UPRT

Another CMVie driving UPRT vector that is proven to label correctly, pcDNA3.3- TOPO-HA-UPRT, was used. It was made by Dr. Chris Doe at the University of Oregon and contains a UPRT gene and a HA tag that can be used for immunostaining as well as western blotting. We have tested TU-tagging using this vector in HeLa cells and P19 cells.

pIRES2-AcGFP1-URA6

The original vector, pIRES2-AcGFP1, has a CMVie promoter and aAcGFP sequence upstream of an IRES sequence. The URA6 sequence was cloned downstream of IRES using the topo cloning method. URA6 is a uridine monophosphate kinase taken from yeast. The URA6 enzyme converts sUMP into sUDP (Figure 8). We chose to overexpress URA6 instead of nucleotide diphosphate kinase (NDK) in the pathway because URA6 is a rate limiting step, and its expression level is more cell type dependent. Originally, this pIRES2-AcGFP1-URA6 vector was going to be co-transfected with a UPRT vector to enhance RNA labeling. Additionally, this vector expresses GFP, therefore the cells can be sorted with FACS and the results would validate the UPRT method.



Figure 8: Pathway from sUMP to sUDP to sUTP.

Although this vector is made and the sequence and orientation are shown to be correct, this vector has not been shown to work in HeLa cells. For the control experiment, lipofectamine

transfection is shown to work when transfected HeLa cells with another GFP vector that were known to work properly (Hernandez-Hoyos, Anderson et al. 2003). However, GFP was not detected with the pEGFP-URA6 transfected HeLa cells. Neither has it been shown to enhance the TU-tagging labeling. For these reasons, the data is not incorporated into this report.

pCMV-Myc-UPRT-2A-HA-UPRT

A vector containing two copies of UPRT, pCMV-Myc-UPRT-2A-HA-UPRT was made by a colleague in our lab (Zer Vue). The 2A sequence codes for a small peptide between two UPRT units after translation. This 2A peptide can be recognized and cleaved, giving two UPRT monomers and has an HA tag. This vector was transfected into HeLa cells twice and into P19 cells once. From these preliminary experiments, this vector has not been shown to give a higher labeling efficiency. One reason could be that there is endotoxin in this plasmid during the midi-prep process. However, using the endotoxin removal kit did not help the labeling efficiency. Therefore, more investigation is needed about this vector.

CELL TYPE-SPECIFIC UPRT EXPRESSION VECTORS

Nestin-HA-UPRT (for NSC-specific mRNAs)

Another type of vector should allow UPRT expression only in the neural stem cells. The vector is driven by a nestin promoter, nestin-UPRT. The original nestin-GFP vector that was used to get the nestin promoter came from Nibedita Lenka from the National Center for Cell Science in India. Nestin is a microfilament and marker found in neural stem cells, but not in mature neurons such as the ones having an axon, astrocytes or oligodendrocytes. Therefore, UPRT is expressed only in the neural stem cells, and their mRNAs will be labeled, purified and analyzed.

The nestin-UPRT vector is made using the Gateway cloning method. From my experiments, the Gateway method is an even faster method than the topo cloning method and has a higher success rate. The Gateway method works as follows. The gene to be inserted (UPRT or a cell type-specific promoter nestin) is amplified using PCR with a primer for the gene. A short attB sequence (~30bp) flanks the primer and therefore is added to the end of a gene during amplification. These attB sequences at both ends of the PCR fragment recombine with the attP sequence of the donor vector (pDONR). This step is called the BP reaction because the recombination sites are attB and attP. The new vector containing the gene is the entry clone. The two entry clones, one contains UPRT another contains nestin, recombine with the destination vector. This step is called the LR reaction because the recombination sites are attL and attR. Two or more entry clones are cloned into a destination vector at the same time. The final vector is an expression vector, containing the promoter of choice and gene of interest. The backbone of the nestin-UPRT expression vector is pcDNA6.2/V5-pL-DEST.

The nestin entry clone and the UPRT entry clone have been sequenced and confirmed to be correct, therefore, the sequence of the final expression vector is correct. Six of these clones have been made and all have been validated using PCR screening. The T7 forward primer (upstream of nestin) and the reversed UPRT attB primer (downstream of UPRT) are used and the total fragment shows a ~3kB band (nestin 2kB, UPRT 735nt, and attB sequences). The band of linearized nestin-UPRT expression vector is 8.2kB. The nestin-UPRT vector has not yet been tested for TU-tagging.

Tuj1-HA-UPRT (for Neuronal-specific mRNAs)

The Tuj1-UPRT was going to be made using the Gateway cloning method. The Tuj1 promoter was amplified off a plasmid obtained from Dr. Fred Gage at the Salk Institute. No information could be provided by the technician who sent the plasmids about the primers, the vector sequence or even the backbone that the cDNA was clone into. Therefore, I had to PCR amplify the Tuj1 fragment from the pseudo-unknown plasmid and this made obtaining a verified copy of the Tuj1 promoter challenging. Eventually I obtained a PCR product corresponding to the Tuj1 promoter as indicated by the size of the PCR product. However the Tuj1-attB fragment has not been verified by sequencing and it has not yet been cloned into the entry vector or the destination vector.

GFAP-HA-UPRT (for Astrocyte-specific mRNAs)

The GFAP plasmid was also obtained from the Gage lab. After we sequenced the GFAP fragment, we realized that the GFAP vector sequence that they sent us did not correspond to the sequence of the plasmids that we received. We eventually amplified the GFAP fragment with an attB site using the same approach as we did for the Tuj1, as indicated by the size of the PCR product. Similarly, it has not been verified by sequencing and it has not yet been cloned into the entry vector or the destination vector.

TU-TAGGING METHODS

After cells were transfected with one of the UPRT vectors and UPRT was being expressed, the cells were incubated in 4TU for four hours. A range of 4TU concentrations was tested to find the optimal concentration that gives the maximal contrast between UPRT labeling and non-UPRT labeling. After 4 hours of incubation, the cells were rinsed with PBS, trypsinized and centrifuged into a pellet.

Trizol was used to lyse the cells pellet and prepare mRNAs. A TU-tagging experiment requires at least one million cells. This corresponds to 3 wells of the 6-well plate. One mL of Trizol was used for every 3 million cells. After 10 minutes of Trizol incubation, chloroform was

added (20% of the original volume) to separate RNA (in the upper colorless phase) from DNA (centered opaque film) and the other contents (the bottom sparkled bright pink color solution). The upper phase was carefully transferred into a new RNase free 1.5mL centrifuge tube. The mRNAs was precipitated using isopropanol, rinsed with ethanol, and dissolved in RNase-free water.

The RNA was cleaned using the RNeasy kit to eliminate background labeling of proteins from cystein binding to biotin. This step also cleans RNase should it still exist from the Trizol preparation and prevents RNA degradation.

Then the RNA was biotinylated with biotin-HPDP at 25°C for two hours. Only labeled RNAs that carry a thio-tag will react with biotin. The excess biotin was removed using chloroform and a phase locked gel column. Then the RNA was precipitated using isopropanol, rinsed with ethanol, and dissolved in RNase free water.

A table top centrifuge run at 4°C was used in all the steps to separate phases and precipitate RNAs. RNAs were stored at -80°C to prevent degradation. To help eliminate RNA degradation, the entire experiments were performed under an RNA designated workstation and on ice. Trizol and chloroform manipulation were performed under the fume hood. The concentration of RNA was measured using a NanoDrop device and confirmed by loading the same weight of samples across the gel.

Northern blot or slot blot can be used to assess TU-tagging efficiency. In the Northern blot, RNA samples were run on a gel. A glass tray was filled with 10x SSC, composed of 175.3g of NaCl and 88.2g of sodium citrate in 800mL of water with a pH of 7.0. A plate was placed across the glass tray. A Whatman paper pre-moistened with SSC was placed around the plate and allowed to uptake liquid from the SSC bath. The loading wells of the gel were cut and the gel is cut smaller according to the lanes being used. The gel was placed on the Whatman paper on the plate. A parafilm was adhered to all the edges of the gel. A Hybond N+ membrane was cut to the size of the gel and placed on the gel. Three pieces of Whatman papers were placed on the membrane. A stack of paper towels cut to the size of the gel was placed on top, followed by a lid from pipet tip box, and a bottle to add weight. The transfer process took 16 hours or more. Since RNA samples were run on a gel and were separated by their size, three bands can be visualized in the Northern blot.

Slot blot is similar to Northern blot in that RNAs were measured on a membrane. The difference is the transferring method onto the membrane, resulting in a different visualization of the blot. In slot-blot, a Bio-Dot apparatus was used to transfer RNA onto the membrane. Three pieces of Bio-Dot filter papers were pre-wet in water and placed on the chamber of the apparatus. A Hybond N+ membrane cut to the same size was pre-wet in 6x SSC for 10 minutes and placed on the filter papers. A sample template containing 8x6 wells was placed on the membrane and was sealed with attached screws. The screws were further tightened while a vacuum pressure is applied. Immediately prior to loading RNA samples on the template, each of the wells was loaded with 100uL of water and a vacuum pressure was applied to re-wet the membrane. The vacuum is turned off immediately when the water on the wells was drained. 1ug of RNA was diluted into a total of 100uL solution for each sample and 0.5uL of loading dye was added. A loading scheme was designed on the 8x6 well-plate prior to loading. The wells

not used for sample loading were loaded with water. Then the RNA samples were loaded as designed on the scheme. A vacuum pressure was applied to transfer the sample onto the membrane. The process was monitored and took 5-15 minutes to ensure complete transfer. The membrane had dye marking where RNA samples were loaded. Since RNA of various sizes was loaded onto one slot, only one band can be visualized on a slot blot.

The RNAs were then crosslinked onto the membrane by exposing the membrane under the UV for 1 minute using Optimal Crosslinking setting of the SpectroLinker XL-1000 UV Crosslinker instrument. Then the membrane was incubated in Blocking solution for 30 minutes to prevent non-specific binding of the Streptavidin. The solution in this and the following steps were held in a pipet tip box and very slowly mixed with a shaker. The solution was replaced with 10mL of Blocking solution that contained Streptavidin-HRP for 5 minutes. The blocking solution is composed of 3.65g NaCl, 1.2g Na₂HPO₄, 0.5g NaH₂PO₄ and 50g SDS dissolved in 500mL water heated to 37°C. Streptavidin-HRP to Blocking solution ratios of 1:500 dilution and 1:100 were tested. The 1:100 dilution gave a better contrast between UPRT labeling and non-specific binding, thus the 1:100 Streptavidin-HRP have been used in the following experiments. The membrane is bound with all RNAs from all kinds of cells, but only those UPRT expressing RNA contain a thio-tag will attached to a biotin, which will then react with Streptavidin-HRP. The excess Streptavidin-HRP was washed twice in Wash I each for 20 minutes, then twice in Wash II each for 5 minutes. The Wash I is a 1:10 dilution from Blocking solution. The 10X stock of Wash II is composed of 6.0g Tris, 2.9g NaCl and 1.0g MgCl₂ in 500mL of water, adjusted to a pH of 9.5. Then the membrane was incubated in 10mL SuperSignal ECL reagents (5mL stable peroxide solution and 5mL luminol enhancer solution) for 5 minutes. The light from the HRP-ECL reaction is recorded using Chemi Hi Sensitivity setting of the Chemi-Dot instrument.

P19 CELL CULTURE AND TRANSFECTION METHODS

RATIONALE

The cells markers and gene expression of P19 neural differentiation show that P19 is a reliable tissue culture model for studying neurogenesis. P19 is a murine embryonal carcinoma cell line. They are immortal and generate new cells for experimental studies indefinitely. When P19 cells are exposed to retinoic acid (RA), they follow the fate of neurogenesis(Jones-Villeneuve, McBurney et al. 1982). The temporal invariant pattern of the P19 neural differentiation recapitulates that of the primary NSCs published in most literature, in that the embryonal-like cells first become NSC-like, then some of the NSC-like cells produce neurons, later these NSC-like cells produce more astrocytes and oligodendrocytes(Shen, Goderie et al. 2004).

P19 neural differentiation has a temporal pattern, which mimics that of the primary NSCs, as shown in both the expression of specific markers and the genome-wide gene expression over time. Principal component analysis of the genome-wide gene expression for different cell types (embryonic stem cells ES 129 and ES R1 and ES N2B27, embryonic carcinoma cell line P19 and

F9, NSCs from adult brain, differentiated neural cells, placenta, and trophoblast stem cells) was performed (Aiba, Sharov et al. 2006). Principle component analysis is decomposition of a large number of potentially dependent variables (thousands of genes) into a small number of independent variables by calculating the eigenvectors (principal components). The first principal component (PC1) captures most of the variation, following PC2, PC3, etc. PC1 in this article represents 4000 genes, among 12,200 total genes. The ES N2B27 neural differentiation trend (d1, d2, d3, d4, d5, d6) moves along the PC1 axis. This suggests that the PC1 axis indicates the neural differentiation commitment. P19 neural differentiation follows the same trend, in that P19 starts at the same position on the PC1 axis as that of the early stage of ES neural differentiation, while four days after RA induction, P19 lands at the same position as d6 of the ES neural differentiation.

P19 NEURAL DIFFERENTIATION

P19 RA neural differentiation protocols have been established although no details are published (Bain, Ray et al. 1994; Shen, Mani et al. 2004; Aiba, Sharov et al. 2006), thus small variation of the experiment is possible. The regular P19 media is composed of low-glucose DMEM, 10% FBS, 1% P/S and 1% L-glutamine. In one of my protocols, P19 cells were seeded on a non-adherent 6-well plate at low density (0.25×10^5 cells / mL, 1×10^5 cells / mL and 3.3×10^5 cells / mL) (Figure 9). The cells form aggregates since they do not adhere to the plate, like embryoid bodies. The aggregate structure alone can direct P19 to acquire a neural fate. 0.25×10^5 cells / mL gave rise to too few cells; 3.3×10^5 cells / mL gave rise to some floating dead cells; and 1×10^5 cells / mL is the best seeding density that gave enough viable cells.

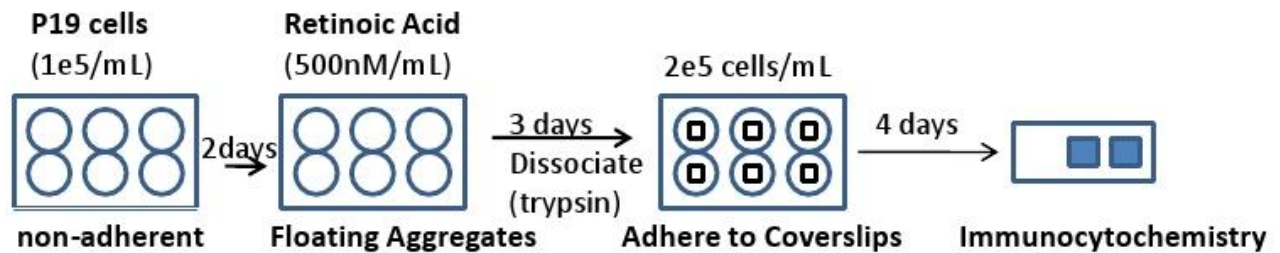


Figure 9: Flow Chart for P19 RA Neural Differentiation and Cell Marker Staining Experiment.

After 2 days of aggregate formation, media was replaced with those containing 500nM/mL of RA. Cell viability was 20% as shown in Trypan blue stain. The low viability mostly likely was due to harsh pipetting, as 95% viability was shown of the same cells at a later time point. The floating aggregates continue to grow and reprogram to adopt a neural fate. Three days later, the cells were transferred to a 15mL conical tube using a 5mL pipette. Aggregates were spun down and washed with PBS. The aggregates were dissociated in 0.25% trypsin-EDTA at 37°C for 8 minutes with gentle mixing every 2 minutes. Two volumes of

serum media were added to inactivate trypsin and aggregates were dispersed by pipetting. The dissociated cells were spun again to remove all RA and trypsin-EDTA, and fed with regular media (described above). The cells had 95% viability.

The cells were plated on ethanol treated glass cover slips placed on 6-well plates. Different densities were compared, 0.1×10^5 cells/mL, 0.5×10^5 cells / mL, 1×10^5 cells/mL, 2×10^5 cells/mL, 4×10^5 cells / mL and 6×10^5 cells / mL, each has one replicate. 2×10^5 cells/mL was the optimal seeding density since it was high enough to promote cell growth and formation, yet low enough that the cells were not too confluent after many days of differentiation. Cells were also grown on regular tissue culture plate with the same density. They had the same morphologies as those grown on cover slips throughout differentiation. After 4 days of differentiation, the cells were fixed with 4% PFA. Fixation with cold methanol was tested and did not affect the results. Immunocytochemistry was used to probe intracellular markers, following a colleague's protocol (Eric Lau, Pallavicini lab). Anti-mouse Texas Red as used as secondary antibody for NSC marker Nestin. Anti-rabbit antibody conjugated with a fluorochrome that fluoresces in the green spectrum was the secondary antibody for neuron marker Tuj1.

UPRT TRANSFECTION

The ubiquitous UPRT vectors (pcDNA3.3- TOPO-HA-UPRT, pIRES-UPRT, pCMV-Myc-UPRT-2A-HA-UPRT) have been tested in HeLa cells and P19 cells. The culture and transfection protocols are identical for HeLa cells and P19 cells. The cells were transfected in a 6-well tissue culture plate (Figure 10). They were seeded at 2×10^5 per well density, adhered and grew. One day later when the cells reach to 50-60% confluency, the UPRT vector was delivered into cells using lipofectamine transfection kit. Cells were maintained in T25 flask, split at 1:20 to 1:100 ratios every 3 days to one week. Cells were multiplied in T75 flask before an experiment. They were then split and plated in 6-well plates. At the end of culturing cells, they were rinsed with PBS, trypsinized and collected into a pellet using a low speed centrifuge.

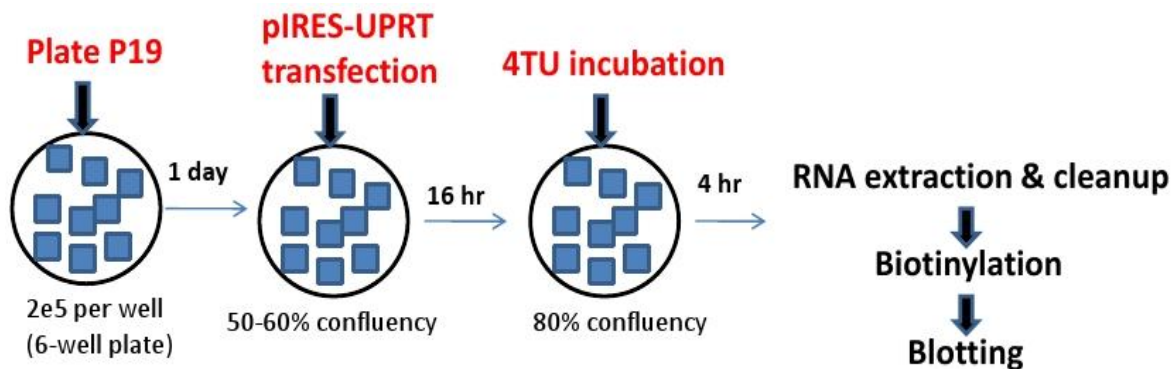


Figure 10: Flow Chart for TU-tagging Experiments in P19 Culture.

CHAPTER 3: RESULTS AND DISCUSSION

TU-TAGGING IN HELA AS CONTROL

The ubiquitous UPRT vectors (pcDNA3.3- TOPO-HA-UPRT, pIRES-UPRT, pCMV-Myc-UPRT-2A-HA-UPRT) were first tested in HeLa cells. The figure below (Figure 11a) shows the loading control of biotinylated RNA, ran on an Ethidium Bromide 1% gel. 0.2 microgram of RNA was loaded on each lane. UPRT+ samples are mRNAs from HeLa cells transfected with pcDNA3.3- TOPO-HA-UPRT. Negative control samples are mRNAs from HeLa cells without UPRT transfection. The lanes represent different concentrations of 4TU (10uM, 25uM, 50uM, 75uM and 100uM).

Figure 11b is a slot-blot of streptavidin-HRP probe. The data suggest that 50uM is the optimal 4TU concentration, since in the 10 minute light detection film the 50uM band has a higher intensity than the 25uM band yet has the same intensity as 75uM and 100uM bands. The same intensity of 50uM, 75uM and 100uM bands are due to detection saturation within 10 min light exposure. In the 40 minute light detection film, the negative control of 50uM band is the same as 25uM and 10uM bands, yet less than 75uM and 100uM bands.

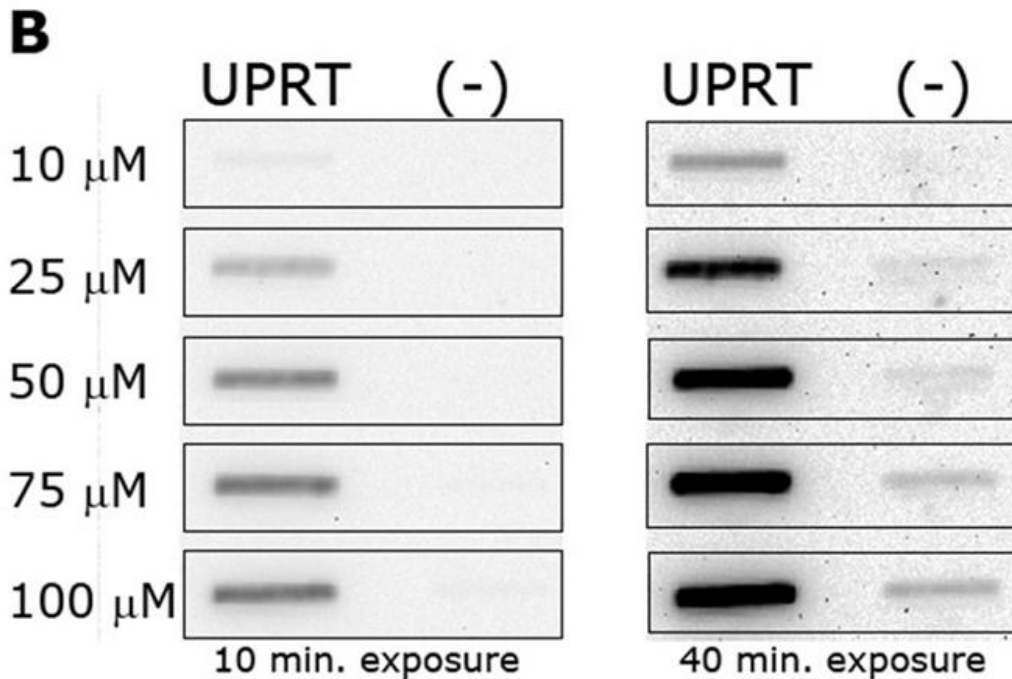
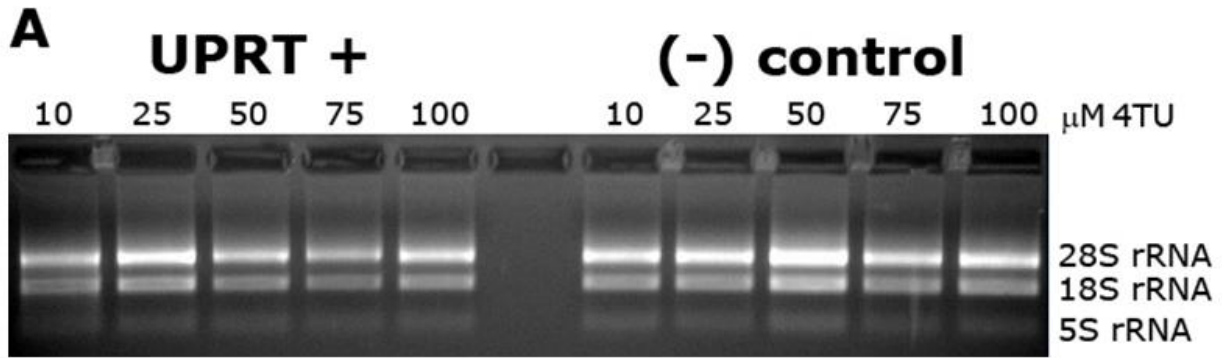


Figure 11: TU-Tagging Blot in HeLa Tissue Culture. Loading control of biotinylated RNA run on an EtBr gel (a). Slot blot comparing five Concentrations of 4TU (10 μM , 25 μM , 50 μM , 75 μM and 100 μM), each for 4 hours (B). Lanes labeled as UPRT were from HeLa cells transfected with pcDNA3.3-TOPO-HA-UPRT.

Lanes labeled as (-) are negative controls where cells were not transfected with UPRT vector but were incubated in 4TU of respective concentrations and time duration. Light from the reaction of Step-HRP and ECL was detected on the film for 10 minutes (left) and 40 minutes (right) of exposure.

Thus, 50 μM of 4TU incubation is the optimal condition for HeLa culture because it gives strong UPRT labeling yet minimal labeling from other biochemical pathways. There are UPRT alternative pathways that incorporate a thio-tag onto the RNAs, but at a much lower rate compared to the UPRT pathway. For example, orotatephosphoribosyltransferase (OPRT) converts uracil to UMP via the *de novo* pyrimidine synthesis pathway, although the activity is

low and occurs only at high pH. Uridine phosphorylase and uridine kinase can sequentially convert uracil to UMP, again at a much lower rate compared to UPRT labeling (Cleary 2008).

TU-TAGGING P19 CULTURE

The ubiquitous pIRES-UPRT expression vector was used for TU-tagging in P19 culture.

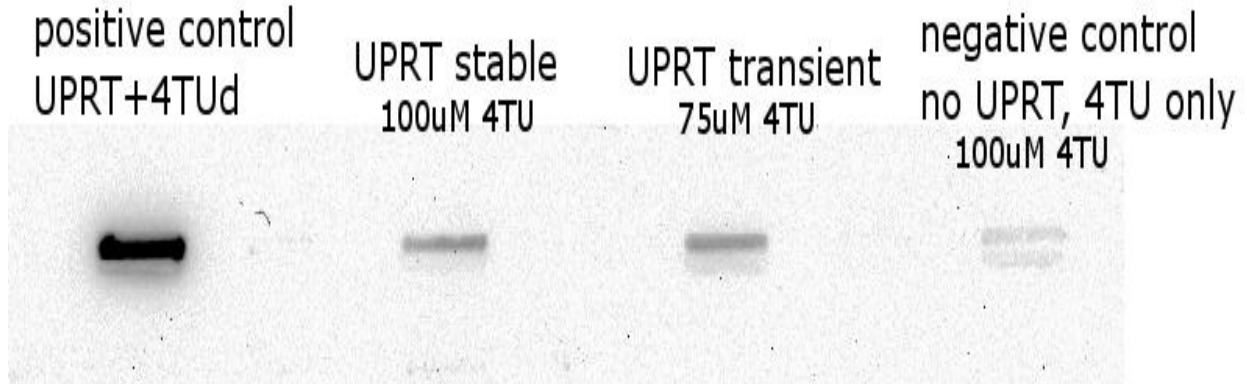


Figure 12: TU-Tagging Blot in P19 Tissue Culture. The first lane is a positive control for biotinylation reaction because 4-thiouridine is incorporated into nascent mRNAs independent of UPRT. The second lane was from cells transfected with pIRES-UPRT and were under drug selection for two months, thus supposedly gave stable UPRT expression. The third lane was from cells transfected with pIRES-UPRT a day prior to 4TU incubation. The fourth lane was from cells not transfected with UPRT vector but were incubated in 4TU.

Figure 12 is a slot blot of TU-tagging in P19 cells using the pIRES-UPRT vector. All RNAs were bound to the membrane, and the band shows detection of thio-tagged RNA. The four bands are RNA from P19 culture under different conditions. The first lane is RNA from P19 cells that were transfected with pIRES-UPRT two months prior to 4-thiouridine (4TUd) incubation for 4 hours. This is a positive control for biotinylation reaction because 4-thiouridine is incorporated into nascent mRNAs independent of UPRT (Figure 5). The 4TUd signal is stronger than the UPRT dependent 4TU signals (second and third lanes), because not all uridine of the mRNAs contains a thio-tag in the latter samples.

The second lane shows mRNA labeling of P19 cells that supposedly express UPRT stably. Cells were transfected with pIRES-UPRT and were under G418 neomycin drug selection for two months. Since pIRES-UPRT vector contains a neomycin resistant gene, transfected cells were resistant to G418 and can survive while non-transfected cells did not survive. The cells were incubated in 4-thiouracil (4TU) for 4 hours prior to RNA extraction.

The third lane shows mRNA labeling of P19 cells that express UPRT transiently. Cells were transfected with pIRES-UPRT a day prior to 4TU incubation for 4 hours. UPRT was given time to express for one day while the cells reached 80% confluency. Then the cells were incubated in 4TU for 4 hours prior to RNA extraction.

The fourth lane shows mRNA of P19 cells that were not transfected with pIRES-UPRT. We call this a negative control or background since any mRNA labeling is not a result of UPRT. The cells were incubated in 4TU with the same concentration as those cells that were transfected with pIRES-UPRT. One ug of total RNA was loaded to each of the four lanes.

Three conclusions can be drawn from these data. First, TU-tagging is successful in P19 cells using pIRES-UPRT transfection. The pcDNA3.3-TOPO-HA-UPRT transfection is successful in P19 cells as well (data not shown). We conclude that TU-tagging works in P19 cells because signals from UPRT expressing cells (both stable and transient) have higher intensity bands than that of the non-UPRT expressing cells (negative control).

Secondly, TU-tagging of cells that have episomal UPRT expression (transient expression) has a higher efficiency than those that were given time to incorporate UPRT gene into their chromosome and were under drug selection for a long period of time (stable expression). Therefore, stable expression (more than one month) is not recommended for TU-tagging in P19 cells using lipofectamine transfection, and transient labeling is perhaps more reliable to obtain RNA for gene expression analysis. Transient transfection is fast for one experiment while stable transfection is more time efficient for multiple experiments and consistency is more likely. Stable transfection does not seem to have a good TU-tagging efficiency in this data.

Alternatively, lentiviruses potentially give more stable UPRT expression since they integrates transgenes into cellular genome and have 100% infection rate (Barkho et al., 2006). Therefore lentiviral transduction should give a higher TU-tagging efficiency for a long time of cell culture without repetitive transfection. Maybe the long-term UPRT expression is harmful to cells, so inadvertently selecting for cells with low expression when make stable line, although this is not the case in previous studies in HeLa cells (Cleary, Meiering et al. 2005) or in *Drosophila* (Miller, Robinson et al. 2009). Immunocytochemistry of P19 cells transfected with pcDNA3.3-TOPO-HA-UPRT which were under drug selection for two months did not show the HA tag (Figure 13C). The HA tag flanks the UPRT sequence in the vector. This implies that UPRT transgene was lost in stable transfection cells. The HA stain was shown in the transient transfection P19 cells (Figure 13B). Neucleotransfection where cells are under an electrical current that delivers the vectors directly into the neuclus, gives a higher HA expression (Figure 13A). However, it does not seem to have a significant difference when comparing transfection of GFP vectors.

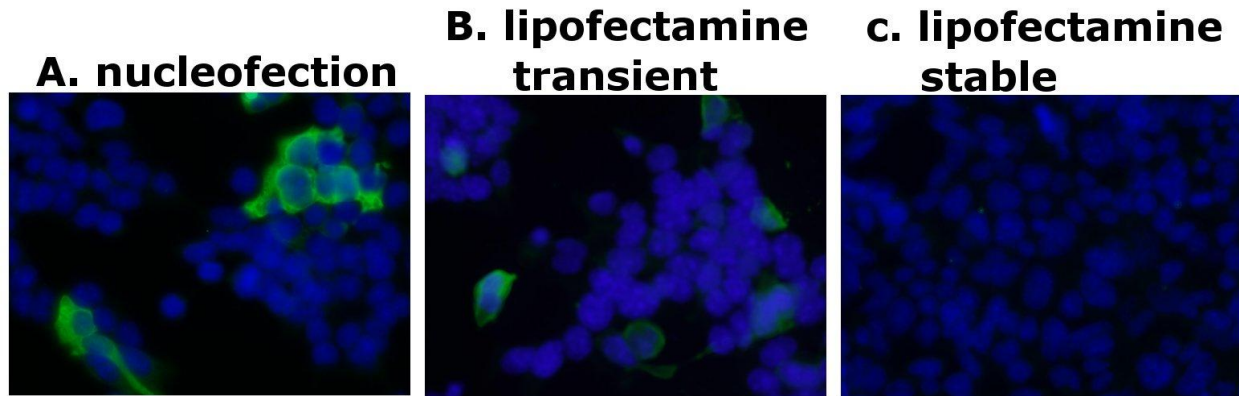


Figure 13: HA staining of pcDNA3.3-TOPO-HA-UPRT transfected P19 cells. A. Transfection by nucleofection method. B. Transfection by lipofectamine method one day before imaged. C. Transfection by lipofectamine method two months before imaged.

Thirdly, TU-tagging background is higher in P19 culture (Figure 12, 4th lane) than in HeLa culture (Figure 11b, negative controls). In both figures, 1 μ g of RNAs are loaded and light acquisition is 40 minutes. HeLa and P19 cells are originated from different species and different developmental stages. The pluripotency of P19 cells may contribute to a higher background. Cancer cell lines have altered metabolism. The enzymes of the UPRT alternative pathways (orotatephosphoribosyltransferase (OPRT), uridinephosphorylase and uridine kinase) are likely to be more elevated in cancerous cells. This may increase the background of P19 cells; therefore, a lower concentration of 4TU should be used to ensure that the thio-tagged mRNAs are cell type-specific. However, there should be less background in primary NSCs; therefore, a higher concentration of 4TU can be incorporated to increase labeling efficiency.

P19 NEURAL DIFFERENTIATION

NSCs and neurons were successfully derived from P19 cells as indicated by immunostaining of cell markers. Figure 14a (top panel) shows the presence of NSCs probed by Nestin antibody (MAB353, mouse monoclonal), the presence of neurons probed by Tuj1 antibody (ab18207, rabbit polyclonal), and all cells (P19 RA differentiation was heterogeneous) by DAPI staining. Neurons of different morphologies were shown in the immunocytochemistry images of this experiment (Figure 14b, top panel). Some had fine tubulin fibers (Figure 14b, top panel, left image), some had pronounced axon projections (Figure 14b, top panel, centered image), and some had less pronounced axon projections (Figure 14b, top panel, right image).

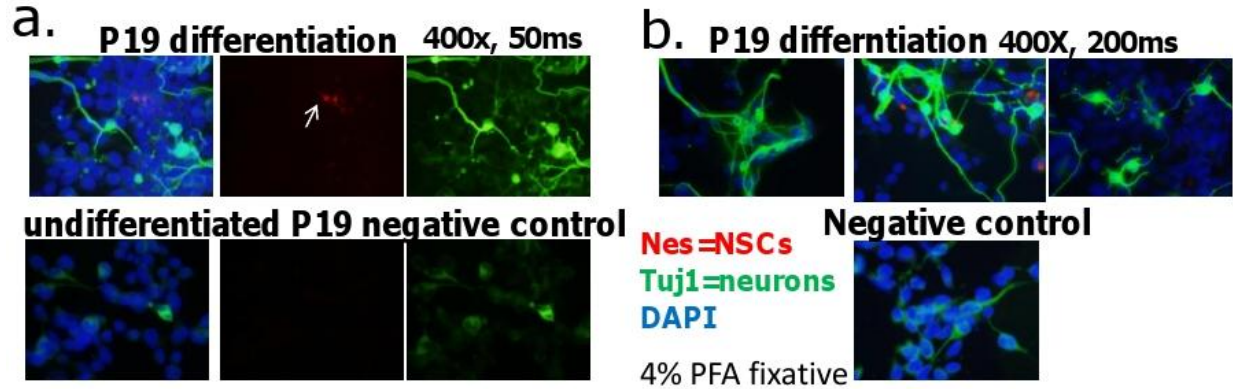


Figure 14: Immunocytochemistry from P19 Neural Differentiation. Three channels of the same field for RA induced differentiation (a,top panel) and negative control where there is no RA induction or aggregate formation (a,bottom panel). Three different fields of the same differentiation experiment showing three channels (b,top) and one field of the negative control showing three channels (b,bottom).

To validate the nestin and Tuj1 markers are cell type-specific, a negative control was performed (Figure 14a and 14b, bottom panels). In the negative control samples, cells were not plated on non-adherent plate nor incubated in RA. They were P19 cells plated directly on cover slips. Different seeding density were tested, $1e5/mL$, $5e5/mL$ and $10e5/mL$, each had a replicate. After one day when the cells were adhered, they were fixed in cold methanol at $-20^{\circ}C$ for 13 minutes. The $5e5/mL$ replicates were used for immunocytochemistry for the negative control. The $10e5/mL$ samples were used for Trypan blue staining and the cells had an average of 95% viability. As shown in the bottom panel of Figure 14a, neither Nestin nor Tuj1 expression were detected, as predicted when P19 cells were not under the cues of neural differentiation.

On average of 7 fields being imaged, P19 under RA differentiation gave 17.3% Nestin positive NSCs and 11.7% Tuj1 positive neurons (Table 2). While for negative control, on average of 5 fields being imaged, there was 0.64% Nestin positive NSCs and 0.94% Tuj1 positive neurons. The higher percentages of the RA induced cells compared to the negative control validate that the antibodies are cell type-specific and thus the data are validated. The presence of Nestin positive cells and Tuj1 positive cells in this experiment confirms that P19 cell culture can be used as an *in vitro* model for neurogenesis.

Table 2: Data on the Frequency of Cell Types from P19 Neural Differentiation

Experiments	Nestin (NSCs)	Tuj1 (neurons)
Differentiation day4 (avg. over 7 fields)	17.3%	11.7%
Negative control (avg. over 5 fields)	0.64%	0.94%
Shen et al. (RA starts day 0)	40%	20%

The differentiation protocol used in these experiments was based on a P19 differentiation protocol used in a previously published genome wide gene expression analysis in P19 cells exposed to RA (Aiba, Sharov et al. 2006). However, this study did not give frequency of each cell type during P19 differentiation. Therefore, a comparison of these experiments with published data using the same protocol cannot be made. Another protocol exposes RA started at day 0 when P19 cells first form aggregates (Shen, Mani et al. 2004). Please note that the different protocols may result in a slight difference in the frequency. Furthermore, only one differentiation time point was compared.

CHAPTER 4: FUTURE DIRECTIONS

TU-TAGGING IN P19 TISSUE CULTURE USING NESTIN-UPRT VECTOR

I have made a nestin-UPRT vector and have tested a protocol that differentiates P19 cells into neural lineages. A future direction upon this project would be to induce P19 differentiation and extract NSC specific mRNAs from the heterogeneous P19-derived population using nestin-UPRT transfection. P19 cells can be differentiated into neural lineages as describe in the Methods. Then they can be plated onto a 6-well plate and transfected with the nestin-UPRT vector using lipofectamine or viral transduction. For transient UPRT expression, 4TU will be incubated a day after transfection (Figure 15). The nestin-UPRT vector that I constructed is a non-viral base vector. P19 cells may be transduced with lentivirus carrying a nestin promoter driving expression of UPRT, although stable expression of nestin and UPRT still need to be validated in P19 cells. If stable expression is feasible, the stable P19 cell line carrying nestin and UPRT transgenes will expedite experiments since NSC specific mRNAs can be extracted after every neural differentiation condition and at appropriate times. One to four days after RA induction is a typical time range when most NSCs are produced. Experiments need to be performed to find the maximal NSC production, which may depend on the P19 culture condition and RA induction protocols.

The nestin-UPRT transfected P19 cells can be harvested and then NSC specific mRNAs can be purified (Cleary, Meiering et al. 2005). The TU-tagging methods can be validated using RT-qPCR. There should be presence of NSC markers (Table 3) and absence of genes that are known to not express in neural progenitors, such as neuron markers, astrocyte markers, oligodendrocyte markers, embryonic stem cell markers SSEA and Oct4, and fibroblast specific protein FSP1. The NSC specific mRNAs can also be used for microarray analysis to discover novel genes that are expressed at high levels during neurogenesis and those during astrogenesis. A potential pitfall of the P19 tissue culture is that it is a cell line and it might be different from primary NSCs. However, as shown in previous literature, principle component analysis comparing different kinds of embryonic derived NSCs, somatic NSCs and P19 derived NSCs follow the same pathway during the progress of differentiation(Aiba, Sharov et al. 2006). Thus, P19 is a reliable model for neurogenesis. Another pitfall of using the P19 culture is that it is a cancer cell line, thus has a high labeling background from UPRT alternative pathways(Cleary 2008). To overcome this pitfall, a range of 4TU concentrations should be tested to find the optimal concentration of 4TU that gives low background yet enough UPRT labeling for the cell of interests.

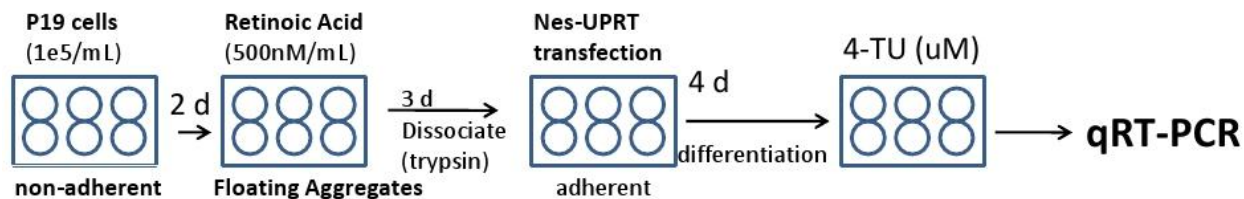


Figure 15: Flow Chart of Future Experiments to Analyze NSC-specific mRNA from P19 Neural Differentiation using Nestin-UPRT Vector.

Table 3: Markers for NSCs, Neurons, Astrocytes and Oligodendrocytes(Composed from Neuromics)

Cell types	Markers
NSCs	A2B5, AP-2 Alpha, Activin RIIA, CD4, CD168/RHAMM, Frizzled 4/CD344, phospho-GAP-43 (S41), Jagged1, Laminin, Mash1, Musashi-1, Nestin , Nestin-1, Nestin-4, Neurofilament alpha-internexin/NF66, Notch1, Notch2, Notch3, Nucleostemin, Otx2, S100B, SOX2 , Semaphorin 3C/6A/6B/7A, TROY/TNFRSF19, Tubulin Beta II, Vimentin.
Neurons	CNPase, Calbindin, ChAT, GAD1/GAD67, HSP105, Ki67, Lingo-1, MAP2 (microtubule assoc protein 2), MARCKS (myristoylated alanine rich C kinase substrate), Mash1, Matrix Metalloproteinase 24, MBP (myelin basic protein), NCAM-L1, NMDA receptor 1 N1, NMDA receptor 2A, Neurofilament NF-H, Neurofilament NF-L, Neurofilament NF-M, Neurofilament alpha-internexin/NF66, Neuron specific enolase (NSE)/ENO2, Neuronal class III β Tubulin (TuJ1), Neurotensin receptor, P11 (calpactin 1 light chain/Annexin II), PGP9.5, PLP (proteolipid protein), PTGDS, RAGE, ROBO1, SCP1, SCP3, Survivin, Synapsin, Synaptojanin 1, Synaptophysin, Synaptosomal associated protein 25/SNAP25, Tau, Tyrosine hydroxylase, UCHL1.
Astrocytes	Coronin 1a/p57, GFAP , HSP105, Survinin, TROY/TNFRSF19, xCT.
Oligodendrocytes	CNPase, GalC , HSP105, MOG, NOGO receptor, Olig1, Olig2 , Olig3, Oligo4, OMgp.

TU-TAGGING IN PRIMARY NSCs AND NICHE CO-CULTURE

In addition to P19 tissue culture, TU-tagging can also be applied to primary NSCs co-cultured with niche cells (endothelial cells and astrocytes). As described in the Introduction, NSCs communicate with their niche cells to maintain homeostasis. Their secreted factors and membrane proteins are extrinsic cues to the NSCs. A future direction would be to compare primary NSCs without niche cells and those with niche cells.

There are many primary cell options for purchasing. Among these are: mouse E14 fetal brain cerebral striatum and mesencephalon (Cell Applications), rat E14 NSCs (Invitrogen), mouse brain endothelial cells (ATCC), primary rat astrocytes (Neuromics), and even healthy adult human brain tissue (Neuromics). For experimental design, rat E14 NSCs from Invitrogen for example, 75% NSCs retain undifferentiated up to three passages (50,000 cells/cm² seeding density, 75-90% passage confluency, reached in 3-4 days), from 2e6 cells to 300e6 cells.

Lentiviral particles containing nestin-UPRT transgenes will be added to the media (Figure 16). The cells will be expanded for two passages, during which time the transgenes will be inserted into the chromosome and give stable expression. Meanwhile, confluent endothelial cell layer or astrocyte layer can be treated with cytosine arabioside (20uM) for 72 hours to eliminate proliferation and recovered in fresh medium for 24 hours (Song, Stevens et al. 2002). On the third passage, NSCs are plated at 10,000 cells/cm² on the niche layer. Co-culture is fed every other day for ten days. They are first fed with undifferentiated media where they adhere and proliferate. The StemPro® NSC SFM Media is specifically formulated for serum-free expansion of human NSCs (Invitrogen). It contains basic FGF recombinant protein and EGF recombinant protein. After 2-3 days when cells are adhered and allowed to proliferate, a different media is fed to guide differentiation. This media does not contain bFGF(Song, Stevens et al. 2002).

Previous literature report that neurons were generated four days after differentiation in either EC niche or astrocyte niche; while astrocytes and oligodendrocytes were generated seven days after (Song, Stevens et al. 2002; Shen, Goderie et al. 2004). However, experiments need to be performed on the cells used to confirm the exact day when the cell type of interests (proliferating NSCs, neurons, or astrocytes) was mostly generated. Since the primary cells are transfected or transduced with cell type-specific promoter UPRT vectors (nestin-UPRT), even if the transfection efficiency is not 100% and there are niche cells, only mRNAs from the NSCs should be present after the purification step if the background from UPRT alternative pathway is low enough. Therefore, having non-transfected cells and niche cells in the population would not affect the results. A report claims that lentivirus has 100% infection efficiency(Barkho, Song et al. 2006)s, therefore, lentivirus should give the best TU-tagging efficiency.

The astrocytes in the niche can either be from the niche cells or are nascent astrocytes differentiated from NSCs. A way to distinguish the two is to transfect a GFAP-GFP vector into NSCs. The niche astrocytes will not have the GFP gene and will not fluoresce. Nascent astrocytes will express GFP as the gene is passed down from the NSCs as they divide and differentiate. This has been shown to work in NSCs (Barkho, Song et al. 2006).

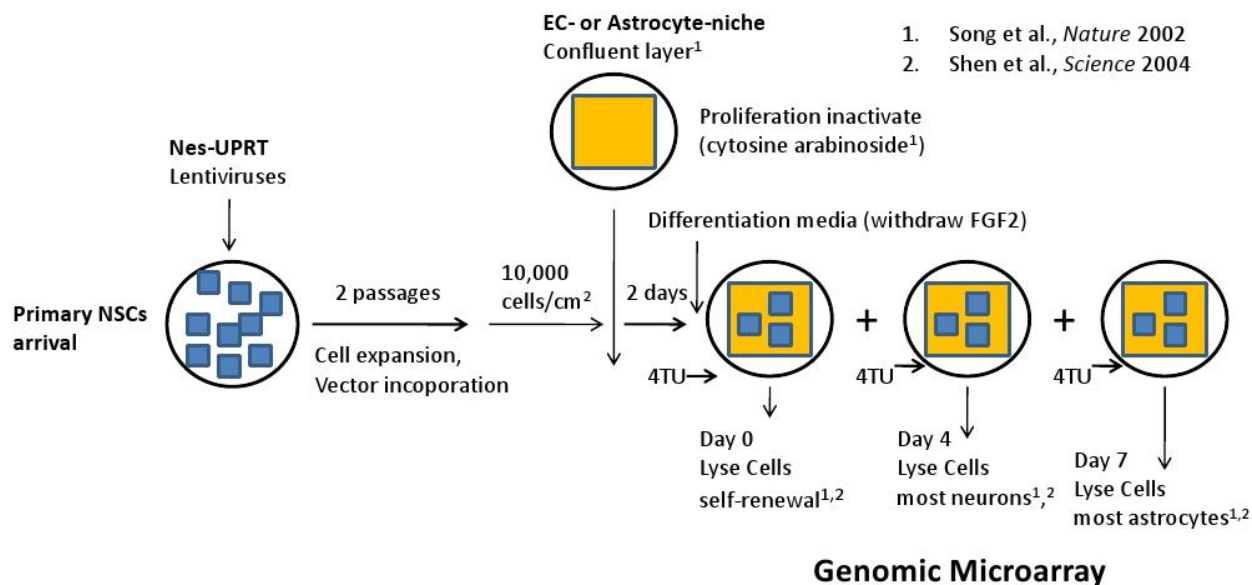


Figure 16: Flow Chart of Future TU-Tagging Experiments on the Co-Culture of Primary NSCs with Endothelial or Astrocyte Niche Cells.

Genomic microarray would be useful to compare the expression level of each gene from NSCs under three different culture conditions: control experiment of NSCs culture alone in the absence of niche cells, primary NSCs co-cultured with ECs niche, primary NSCs co-cultured with astrocytes niche. Since the mRNAs are from neural cells, transcription factors that have high expression levels are likely to be involved in neurogenesis. They can be compared for these three conditions. I have not done microarray analysis, but I have found some references (Aiba, Sharov et al. 2006) (Luo, Schwartz et al. 2006) (Porter, Olson et al. 2009). This would help validate or invalidate our hypothesis that there are more transcription factors that determine NSC neural-fate and, astrocyte-fate when NSCs communicate with their niche cells.

REFERENCES

- Aiba, K., A. A. Sharov, et al. (2006). "Defining a developmental path to neural fate by global expression profiling of mouse embryonic stem cells and adult neural stem/progenitor cells." *Stem Cells* **24**(4): 889-895.
- Bain, G., W. J. Ray, et al. (1994). "From embryonal carcinoma cells to neurons: the P19 pathway." *Bioessays* **16**(5): 343-348.
- Barkho, B. Z., H. Song, et al. (2006). "Identification of astrocyte-expressed factors that modulate neural stem/progenitor cell differentiation." *Stem Cells Dev* **15**(3): 407-421.
- Cheng, L. C., E. Pastrana, et al. (2009). "miR-124 regulates adult neurogenesis in the subventricular zone stem cell niche." *Nat Neurosci* **12**(4): 399-408.
- Cleary, M. D. (2008). "Cell type-specific analysis of mRNA synthesis and decay in vivo with uracil phosphoribosyltransferase and 4-thiouracil." *Methods Enzymol* **448**: 379-406.
- Cleary, M. D., C. D. Meiering, et al. (2005). "Biosynthetic labeling of RNA with uracil phosphoribosyltransferase allows cell-specific microarray analysis of mRNA synthesis and decay." *Nat Biotechnol* **23**(2): 232-237.
- Colombo, E., S. G. Giannelli, et al. (2006). "Embryonic stem-derived versus somatic neural stem cells: a comparative analysis of their developmental potential and molecular phenotype." *Stem Cells* **24**(4): 825-834.
- Gaspard, N., T. Bouchet, et al. (2008). "An intrinsic mechanism of corticogenesis from embryonic stem cells." *Nature* **455**(7211): 351-357.
- Giese, A. K., J. Frahm, et al. (2010). "Erythropoietin and the effect of oxygen during proliferation and differentiation of human neural progenitor cells." *BMC Cell Biol* **11**(1): 94.
- Heiman, M., A. Schaefer, et al. (2008). "A translational profiling approach for the molecular characterization of CNS cell types." *Cell* **135**(4): 738-748.
- Hernandez-Hoyos, G., M. K. Anderson, et al. (2003). "GATA-3 expression is controlled by TCR signals and regulates CD4/CD8 differentiation." *Immunity* **19**(1): 83-94.
- Hwang, D. H., B. G. Kim, et al. (2009). "Transplantation of human neural stem cells transduced with Olig2 transcription factor improves locomotor recovery and enhances myelination in the white matter of rat spinal cord following contusive injury." *BMC Neurosci* **10**: 117.
- Islam, M. S., K. Tatsumi, et al. (2009). "Olig2-expressing progenitor cells preferentially differentiate into oligodendrocytes in cuprizone-induced demyelinated lesions." *Neurochem Int* **54**(3-4): 192-198.
- Jacob, J., C. Maurange, et al. (2008). "Temporal control of neuronal diversity: common regulatory principles in insects and vertebrates?" *Development* **135**(21): 3481.
- Jones-Villeneuve, E. M., M. W. McBurney, et al. (1982). "Retinoic acid induces embryonal carcinoma cells to differentiate into neurons and glial cells." *J Cell Biol* **94**(2): 253-262.
- Kriegstein, A. and A. Alvarez-Buylla (2009). "The glial nature of embryonic and adult neural stem cells." *Annu Rev Neurosci* **32**: 149-184.
- Lie, D. C., H. Song, et al. (2004). "Neurogenesis in the adult brain: new strategies for central nervous system diseases." *Annu Rev Pharmacol Toxicol* **44**: 399-421.
- Luo, Y., C. Schwartz, et al. (2006). "A focused microarray to assess dopaminergic and glial cell differentiation from fetal tissue or embryonic stem cells." *Stem Cells* **24**(4): 865-875.

- Miller, F. D. and A. Gauthier-Fisher (2009). "Home at last: neural stem cell niches defined." Cell Stem Cell **4**(6): 507-510.
- Miller, M. R., K. J. Robinson, et al. (2009). "TU-tagging: cell type-specific RNA isolation from intact complex tissues." Nat Methods **6**(6): 439-441.
- Parker, M. A., J. K. Anderson, et al. (2005). "Expression profile of an operationally-defined neural stem cell clone." Exp Neurol **194**(2): 320-332.
- Samuels, I. S., J. C. Karlo, et al. (2008). "Deletion of ERK2 mitogen-activated protein kinase identifies its key roles in cortical neurogenesis and cognitive function." J Neurosci **28**(27): 6983-6995.
- Shen, Q., S. K. Goderie, et al. (2004). "Endothelial cells stimulate self-renewal and expand neurogenesis of neural stem cells." Science **304**(5675): 1338-1340.
- Shen, Y., S. Mani, et al. (2004). "Failure to express GAP-43 leads to disruption of a multipotent precursor and inhibits astrocyte differentiation." Mol Cell Neurosci **26**(3): 390-405.
- Song, H., C. F. Stevens, et al. (2002). "Astroglia induce neurogenesis from adult neural stem cells." Nature **417**(6884): 39-44.
- Suhonen, J. O., D. A. Peterson, et al. (1996). "Differentiation of adult hippocampus-derived progenitors into olfactory neurons in vivo." Nature **383**(6601): 624-627.
- Svendsen, C. N. and A. G. Smith (1999). "New prospects for human stem-cell therapy in the nervous system." Trends Neurosci **22**(8): 357-364.
- Wurmser, A. E., T. D. Palmer, et al. (2004). "Neuroscience. Cellular interactions in the stem cell niche." Science **304**(5675): 1253-1255.
- Xiao, Q., Y. Du, et al. (2010). "Bone morphogenetic proteins mediate cellular response and, together with Noggin, regulate astrocyte differentiation after spinal cord injury." Exp Neurol **221**(2): 353-366.